Bed turbulent kinetic energy boundary conditions for trapping efficiency and spatial distribution of sediments in basins

Gilles Isenmann, Matthieu Dufresne, José Vazquez and Robert Mose

ABSTRACT

The purpose of this study is to develop and validate a numerical tool for evaluating the performance of a settling basin regarding the trapping of suspended matter. The Euler-Lagrange approach was chosen to model the flow and sediment transport. The numerical model developed relies on the open source library OpenFOAM®, enhanced with new particle/wall interaction conditions to limit sediment deposition in zones with favourable hydrodynamic conditions (shear stress, turbulent kinetic energy). In particular, a new relation is proposed for calculating the turbulent kinetic energy threshold as a function of the properties of each particle (diameter and density). The numerical model is compared to three experimental datasets taken from the literature and collected for scale models of basins. The comparison of the numerical and experimental results permits concluding on the model's capacity to predict the trapping of particles in a settling basin with an absolute error in the region of 5% when the sediment depositions occur over the entire bed. In the case of sediment depositions localised in preferential zones, their distribution is reproduced well by the model and trapping efficiency is evaluated with an absolute error in the region of 10% (excluding cases of particles with very low density).

Key words | computational fluid dynamics (CFD), particle tracking, sediment deposition, sediment transport, suspended matter

Gilles Isenmann (corresponding author)
Matthieu Dufresne
José Vazquez
Robert Mose
National School for Water and Environmental Engineering of Strasbourg (ENGEES),
1 quai Koch,
Strasbourg 67000,
France
and
Mechanics Department, Fluid Mechanics Team,
ICube (University of Strasbourg, CNRS, INSA of Strasbourg, ENGEES),
2 rue Boussingault,
Strasbourg 67000,
France
E-mail: *gilles.isenmann@engees.unistra.fr*

INTRODUCTION

Runoff water transported in drainage networks can carry substances harmful for aquatic environments (organic matter, metals, fuels, etc.). A fraction of this pollution is fixed on suspended matter (SM) (Ashley *et al.* 2004). To limit pollution discharged in the receiving medium, different systems have been installed at the outlets of networks with the overall objective of trapping SM by settling. The size of these structures can vary from several cubic metres, for lamella and dynamic settlers, to several tens of thousand cubic metres for storage basins. Despite the intensive use of these systems, often little is known of how they function and their settling efficiency is estimated using dimensioning rules based on Hazen's sedimentation theory (Jarrell-Smith & Friedrich 2011). However, the flow can have very different forms according to the geometry of the structure considered: horizontal or vertical, and symmetrical or asymmetrical recirculations (Dewals *et al.* 2008; Dufresne *et al.* 2009). In this case, Hazen's sedimentation theory can prove to be uncertain, as it is used outside its scope of application, and another method must be used to evaluate the efficiency of the structure more precisely.

Several solutions are available. An evaluation can be performed on site by instrumenting the installation to measure turbidity and by taking samples at the inlet and outlet of the system, for example (Torres 2008). Nonetheless, this evaluation can only be done once the structure has been built, and its implementation is poorly adapted to the dimensioning phase. It is also possible to study the operation of a settling basin in the laboratory (Adamsson *et al.* 2005). However, setting up this type of system can be expensive and is limited to small structures and scale models. On the contrary, experimental data collected on site or in the laboratory are essential for validating 3D numerical models, another solution for evaluating the operation of a structure at lower cost. Consequently, this article focuses on the development and validation of a methodology

doi: 10.2166/wst.2017.373

based on numerical modelling to predict the performances of a settling basin for design purposes.

The movement of a number of solid particles in a fluid can be modelled by two methods: the Euler-Euler approach and the Euler-Lagrange approach. In the Euler-Euler approach, the fluid phase and the particle phase are considered as continuous phases and are modelled with Navier-Stokes equations. In the case of the Euler-Lagrange approach, the Navier-Stokes equations are still resolved for the fluid phase and Newton's equation of movement is used to determine the trajectory of each particle within the flow (Maxey & Riley 1983). Since the concentration of SM in runoff water is mostly lower than 1 g/l (Ashley *et al.* 2004), the particle phase does not influence the flow and the hydrodynamic calculation can be uncoupled from the movement of particles (Graf & Altinakar 2000). The uncoupled Euler-Lagrange approach was employed successfully in several studies to reproduce particle trapping efficiency in a basin and the distribution of sediment depositions on the bottom (Adamsson *et al.* 2003; Dufresne *et al.* 2009; Yan *et al.* 2014). This approach is used in the present study.

LITERATURE REVIEW

The Euler-Lagrange approach

Hydrodynamic modelling in basins is well mastered. A RANS approach (Versteeg & Malalasekera 2007) coupled with a k-ε type turbulence model and its variants suffices to reproduce the diversity of the types of flows occurring in basins (Stovin & Saul 1996; Dufresne *et al.* 2010). Regarding the modelling of sediment transport, calculating the trajectory of a particle, knowing the forces exerted on it (Maxey & Riley 1983), is also well mastered (Adamsson *et al.* 2003; Dufresne *et al.* 2009; Yan *et al.* 2014). The main difficulty relating to this type of model resides in the boundary condition used to take into account the deposition and the resuspension of a particle that has reached the bottom wall.

Particle/wall interaction

The simplest interaction conditions are *stick* and *rebound* conditions (OpenFOAM 2016). For a *stick* type condition, a null velocity is fixed for the particle coming into contact with the wall and the calculation of its trajectory stops. For a rebound type condition, the particle is resuspended in the flow using an elastic collision equation. These conditions can nonetheless prove to be poorly adapted for representing sediment depositions on the bottom of a basin. Indeed, no sediment deposition is possible with a rebound condition, whereas using a *stick* condition can lead to an overestimation of deposits since any particle reaching the bottom remains deposited (Stovin & Saul 1998). New conditions were therefore proposed to limit sediment depositions to zones with favourable hydrodynamic conditions. All these conditions are based on the same idea of comparing a local hydrodynamic parameter with a threshold value.

Adamsson *et al.* (2003) used shear stress on the bed as a hydrodynamic parameter (BSS for Bed Shear Stress condition). The threshold value selected was evaluated at about 0.03 N/m^2 by Stovin & Saul (1994) on the basis of experiments on a scale model of a basin. The use of this BSS condition led to major improvements in terms of representing zones of sediment deposition in comparison to a stick condition. It should nonetheless be noted that the threshold value used is only valid *a priori* for the scale model and the particles studied experimentally by Stovin & Saul (1994) and numerically by Adamsson *et al.* (2003).

Another approach was proposed by Dufresne *et al.* (2009). It is based on thresholding the turbulent kinetic energy close to the bed (BTKE for Bed Turbulent Kinetic Energy condition). Based on experiments conducted on a small scale laboratory model, the authors identified the range 1.10^{-4}–3.10^{-4} m^2/s^2 for the threshold value of turbulent kinetic energy. The sediment depositions simulated with the BTKE condition showed good consistency with the sediment depositions observed, and provided a better description in comparison to a BSS condition. Yan *et al.* (2014) applied a BTKE condition to reproduce sediment depositions in a large structure (32,000 m^3). The authors determined a threshold value around 10 times lower than that highlighted by Dufresne *et al.* (2009), Yan *et al.* (2014), then proposed the relation $k_c = \xi v_s^2$ to determine the critical turbulent kinetic energy, with ξ being the adjustment coefficient and v_s being the settling velocity representative of the sample. The authors obtained highly satisfactory results by considering a coefficient ξ equal to 1 and a settling velocity $v_{s,80}$ (percentile 80 of the distribution of settling velocities).

For both the BSS and BTKE conditions, the threshold values proposed were adjusted experimentally for a given basin and a sample of particles, making it difficult to transpose them to other configurations. Therefore it would be interesting to obtain a relation that permits the calculation of the threshold value associated with each particle as a function of its properties (diameter and density).

Analogy with channels

Many studies have been performed on sediment transport in channels and rivers. Two modes of transport can be distinguished for lightly loaded flows: bed load and suspension (Van Rijn 1984a). The movement by bed load of a particle at rest on the bed of a canal is classically based on thresholding the shear stress using the Shields diagram (Buffington 1999). Several authors (Brownlie 1981; Van Rijn 1984b) proposed analytical relations to calculate the shear stress of movement using the properties of the particles and the fluid. In particular, Brownlie (1981) proposed Equation (1) to determine the dimensionless critical shear stress θ_c (Equation (2)) as a function of the dimensionless diameter of the particle d^* (Equation (3))

$$\theta_c = 0.22\, d^{*-0.9} + 0.06 \times 10^{-7.7\, d^{*-0.9}} \tag{1}$$

$$\theta_c = \frac{\tau_c}{\left(\rho_p - \rho\right) g d_p} \tag{2}$$

$$d^* = d_p \left[\frac{\rho\left(\rho_p - \rho\right) g}{\mu^2}\right]^{1/3} \tag{3}$$

where τ_c is the critical shear stress; ρ_p is the density of the particle; ρ is the density of the fluid; g is the acceleration of gravity; and d_p is the diameter of the particle.

When the critical shear stress is exceeded, the particles move initially via bed load close to the bed. Sediment transport occurs when turbulent bursts form and become large enough to maintain the particles in suspension in the flow (Van Rijn 1984b). Several criteria can be used to characterise the start of suspension. They permit evaluating the friction velocity threshold $u_c{}^* = (\tau_c/\rho)^{1/2}$ above which suspension becomes significant. Generally, these criteria are expressed in the generic form

$$\frac{u_c^*}{w_s} = \gamma \tag{4}$$

where w_s is the settling velocity of the particle; and γ is the constant or variable parameter according to the authors. The Bagnold criterion corresponds to a constant value of γ equal to 1. The formulation proposed by Van Rijn (1984b) introduces d^* and is expressed by $u_c{}^*/w_s = 4/d^*$ for $1 < d^* < 10$, and $u_c{}^*/w_s = 0.4$ for $d^* > 10$.

Finally, the idea chosen in the present study is to use the formulations obtained in channels as the basis for creating new conditions of interaction between the particles and the bottom walls that are adapted to cases of basins. The aim is to develop a numerical model based on the Euler-Lagrange approach, enriched with new conditions of interaction of BSS and BTKE type using the properties of the particles. The model is then compared to experimental data obtained from the literature to identify the most pertinent condition for reproducing particle trapping efficiency in a basin and the location of sediment deposits on the bottom.

MATERIALS AND METHOD

Numerical model

Hydrodynamics

The movement of the fluid is described by Navier-Stokes equations (Versteeg & Malalasekera 2007). For an incompressible fluid, these equations are expressed by a mass conservation equation and a momentum conservation equation. Water and air flows are described using the *Volume of Fluid* method (Hirt & Nichols 1981) by considering only one fluid whose properties (density and viscosity) vary linearly with the volume fraction α. This parameter is a marker of value 1 in the water phase and 0 in the air phase. It is calculated by resolving a transport equation (Rusche 2002).

The flows considered in this study are turbulent. The Navier-Stokes equations are averaged with time by applying a Reynolds decomposition for the instantaneous velocity and pressure (Versteeg & Malalasekera 2007), and a turbulence model is used to describe the effect of the velocities fluctuating over the mean flow. The k-ω SST model (Shear Stress Transport) with a standard wall function is chosen. The resolution of these equations is done using the *interFoam* solver (Rusche 2002), available in the library OpenFOAM® (OpenFOAM 2016). A full description of this solver is provided in Deshpande *et al.* (2012).

Sediment transport

The trajectory of a particle in a fluid is described from the Lagrangian viewpoint by resolving the Newton equation (Equation (5)). Knowing the sum of the forces acting on the particle, it is possible to determine the evolution of its position and velocity, in other terms, its trajectory (Maxey & Riley 1983).

$$m_p \frac{d\boldsymbol{u_p}}{dt} = \boldsymbol{F_D} + \boldsymbol{F_g} + \boldsymbol{F_a} \tag{5}$$

where m_p is the mass of the particle; $\boldsymbol{u_p}$ is the velocity of the particle; $\boldsymbol{F_D}$ is the drag force; $\boldsymbol{F_g}$ is the apparent weight; and $\boldsymbol{F_a}$ is the additional forces (pressure gradient, added mass force).

The drag force is expressed as

$$F_D = \frac{3}{4}\frac{\rho}{\rho_p}\frac{m_p}{d_p}C_D(\boldsymbol{u}-\boldsymbol{u_p})|\boldsymbol{u}-\boldsymbol{u_p}| \quad (6)$$

with ρ being the density of the fluid; ρ_p being the density of the particle; d_p being the diameter of the particle; C_D being the drag coefficient; and $\boldsymbol{u}$ being the velocity of the fluid.

The drag coefficient C_D is a function of the particle Reynolds number R_p, defined such that $R_p = \rho d_p|\boldsymbol{u}\text{-}\boldsymbol{u_p}|/\mu$ where μ is the dynamic viscosity of water. For low R_p ($R_p < 0.1$), the coefficient C_D is expressed by $C_D = 24/R_p$. For high R_p ($R_p > 1{,}000$), the coefficient is constant and is equal to 0.44. For intermediate particle Reynolds numbers ($0.1 < R_p < 1{,}000$), the coefficient C_D is expressed by Equation (7).

$$C_D = \frac{24}{R_p}\left(1+\frac{1}{6}R_p^{\frac{2}{3}}\right) \quad (7)$$

The apparent weight of a particle $\boldsymbol{F_g}$ corresponds to the force due to the reduced gravity of buoyancy linked to the surrounding fluid. It is expressed by $\boldsymbol{F_g} = m_p\ \boldsymbol{g}\ (1-\rho/\rho_p)$ where $\boldsymbol{g}$ = the gravity acceleration. The additional forces $\boldsymbol{F_a}$ are not detailed here as they are not taken into account in what follows due to their negligible impact on the trajectory (Dufresne *et al.* 2009).

The velocity of the fluid $\boldsymbol{u}$ in Equation (6) corresponds to the instantaneous velocity, whereas the result of a hydrodynamic simulation using the RANS method provides an average velocity $\boldsymbol{U}$. Using the mean velocity to calculate the trajectories amounts to neglecting the turbulent nature of the flow. However, turbulence has the effect of diverting the particles from their trajectories and even of trapping them in eddies for a certain period of time. These phenomena are therefore not negligible. Following the use of a RANS model, the turbulent nature of the flow can be taken into account by using a random walk model to model the turbulent dispersion of particles. Eddies are created randomly and affect the trajectory of the particles. In practice, a local fluctuation component $\boldsymbol{u'}$ is added to the mean velocity of the fluid $\boldsymbol{U}$ at the point where the particle is located. The velocity used to calculate the trajectories is therefore $\boldsymbol{u} = \boldsymbol{U} + \boldsymbol{u'}$. The fluctuating component is estimated by $|\boldsymbol{u'}| = \varphi\ (2k/3)^{0.5}$ where φ is the random number generated from a Gaussian distribution of mean 0 and variance 1; and $(2k/3)^{0.5}$ is the quadratic mean of the fluctuations of the fluid velocity for an isotropic turbulence. The direction of the fluctuating velocity is also generated randomly. The algorithm used is available in the sources (OpenFOAM 2016).

The fluctuating value $\boldsymbol{u'}$ is recalculated at every time step of the correlation t_{turb} and is maintained constant otherwise. The correlation time is calculated using the model proposed by Amsden *et al.* (1989) by $t_{turb} = \min(1/\omega; c_{ps}\,k^{0.5}/(\omega\,|\boldsymbol{U}+\boldsymbol{u'} - \boldsymbol{u_p}|))$ where k and ω are the turbulent variables of the model k-ω SST; and c_{ps} is the empirical constant, equal to 0.16432. The first term in the parenthesis corresponds to the lifetime of the eddy and the second represents the time required for the particle to cross the eddy.

New particle/wall interaction conditions

The BSS and BTKE type conditions are pertinent for modelling the behaviour of the particles close to the bottom of the basin. The threshold values to be selected are, on the other hand, still subject to debate (Adamsson *et al.* 2003; Dufresne *et al.* 2009; Yan *et al.* 2014). A new method, on the scale of the particle, is proposed to calculate the threshold values τ_c (for the BSS condition) and k_c (for the BTKE condition). They are calculated for each particle as a function of their physical properties, such as diameter, density and settling velocity.

BSS condition

The BSS condition is based on the comparison of the shear stress at the wall with a threshold stress τ_c. The threshold value is calculated for each particle as a function of its dimensionless diameter d^* (Equation (3)) by using the interpolation of the Shields diagram proposed by Brownlie (1981) (Equation (1)). This condition is called 'Brownlie BSS' in the rest of the paper.

BTKE condition

Obtaining a relation. The relation used to calculate the turbulent kinetic energy threshold k_c is deduced from the criteria used to characterise the beginning of suspension in channels (Equation (4)). The friction velocity is, by definition

$$u_c^* = \sqrt{\frac{\tau_c}{\rho}} \quad (8)$$

In addition, the shear stress can be expressed as a linear function of the turbulent kinetic energy (Pope *et al.* 2006) by the relation

$$\tau_c = \rho C k_c \tag{9}$$

where C is the constant close to 0.20.

By combining Equations (8) and (9) and by introducing them in Equation (4), we obtain a relation between the turbulent kinetic energy threshold and the settling velocity of the particle: $k_c = \gamma^2 \cdot {w_s}^2 / C$. By posing $\xi = \gamma^2 / C$, we obtain

$$k_c = \xi w_s^2 \tag{10}$$

Contrary to the formulation of Yan *et al.* (2014), parameter ξ is not an adjustment coefficient. It is deduced from the criteria characterising the suspension of particles in a channel. Using Bagnold's criterion ($\gamma = 1$), we obtain a constant value of ξ equal to 5. The Van Rijn criterion (1984b) involves a value of ξ that varies as a function of the dimensionless diameter d^* so that

$$\xi = \frac{80}{d^{*2}} \tag{11}$$

for $1 < d^* < 10$, and $\xi = 0.8$ for $d^* > 10$.

Extension of the Van Rijn criterion. Using the Van Rijn (1984b) criterion, parameter ξ is not defined for the $d^* < 1$. Two possibilities will be investigated for the extension. The first consists of conserving Equation (11) for the $d^* < 1$. This condition will be called 'Van Rijn BTKE' in the rest of the paper. The second is based on the estimation of the value of ξ using the Shields diagram (Equation (1)) and Equations (9) and (10). The settling velocity w_s is calculated using the Stokes formula (Jarrell-Smith & Friedrich 2011), which is valid for the particles considered here ($d^* < 2$). The choice of using the Shields diagram for $d^* < 2$ is justified, since the criteria that characterise the start of bed load and suspension are confounded for this range of d^* (Van Rijn 1984b). Curve $\xi = 320/d^{*4}$ provides an acceptable approximation for the d^* between 0.1 and 2.5. To ensure the continuity in the calculation of ξ, the following relations are proposed: $\xi = 320/d^{*4}$ for $0.1 < d^* < 2$, $\xi = 80/d^{*2}$ for $2 < d^* < 10$, and $\xi = 0.8$ for $d^* > 10$. This condition will be called 'extended Van Rijn BTKE' in the rest of the paper.

Calculation of the settling velocity. The settling velocity of a particle w_s used in Equation (10) is calculated by resolving the system formed by the following equations by iterations:

$$\frac{w_s}{\sqrt{\left(\left(\rho_p/\rho\right) - 1\right) g d_p}} = \sqrt{\frac{4}{3C_D}}$$

$$Re_p = \frac{\rho d_p w_s}{\mu}$$

$$C_D = A_1 + \frac{A_2}{Re_p} + \frac{A_3}{Re_p^2}$$

where A_1, A_2, A_3 are the constants whose values depend on Re_p (Morsi & Alexander 1972).

EXPERIMENTS

The methodology is applied to three series of experiments performed on scale models of basins by Frey *et al.* (1993), Stovin & Saul (1994) and Dufresne *et al.* (2009). The comparison of the numerical results with the experimental measurements makes it possible to verify the model's capacity to reproduce the phenomena involved in the sediment transport in the basin on the basis of two data: particle trapping efficiency in the structure and the preferential zones of sediment deposition on the bottom. The three series of experiments present the characteristics that allow applying the model to a wide range of particles and hydraulic configurations. The parameters of the experiments are summarised in Table 1. These experiments correspond to calmed though nonetheless turbulent flows.

The experiments performed by Frey *et al.* (1993) led to validating the model for hydraulic conditions in which sediment deposit could occur over the whole bed of the

Table 1 | Parameters of experimental data sets from literature

Experiments	Frey *et al.* (1993)	Stovin & Saul (1994)	Dufresne *et al.* (2009)
Froude numbers	0.01–0.05	0.01–0.06	0.002–0.03
Reynolds numbers	4,400–4,800	4,400–16,500	1,300–7,000
ρ_p/ρ	2.650	1.453	1.034
d^*_{50}	1.3; 1.5; 1.8; 2.1; 2.5	0.77	5.12
Sediment deposits	Over the whole bed	In localised zones	In localised zones

structure. The main aim is therefore to verify the model's capacity to reproduce the structure's particle trapping efficiency. In the experiments performed by Stovin & Saul (1994), the hydrodynamic conditions were such that zones without any sediment deposits appeared on the bottom of the basin. The sample of particles used covered a d^* between 0.15 and 2.5, thus, in addition to the trapping efficiency, these experiments are well-adapted to study the new particle/wall interaction conditions, in particular the extension of the Van Rijn (1984b) criterion for small d^* ($d^* < 2$). In the experiments of Dufresne *et al.* (2009), the dimensionless diameters d^* of the particles used were between 2.5 and 10. As with the experiments of Stovin & Saul (1994), the hydrodynamic conditions in the basin were such that sediment depositions were not possible in certain zones. These experiments therefore permit studying the pertinence of the particle/wall interaction conditions for the largest d^* ($d^* > 2$).

The experiments of Frey *et al.* (1993)

Experimental protocol and results. The experiments conducted by Frey *et al.* (1993) focused on the transport of sand particles in four scale models of settling basins. The geometric and hydraulic configurations studied are based on a Froude similitude in comparison to vineyard settling ponds (scale 1/8). The details of the shape and dimensions of the structure can be found in Frey *et al.* (1993). Two discharges (1.1 and 2.2 l/s) were tested at the inlet of the structure. For each of the geometric and hydraulic combinations, five sediment transport experiments were performed, each corresponding to a sample of fine sand. The sand samples were characterised by the median diameter of the grain size distribution ($d_{50} = 51$; 60; 70; 84; 101 μm). Finally, the outgoing percent (equal to the exiting mass divided by injected mass) was evaluated for each experiment. The efficiency (equal to the settled mass divided by the injected mass) is presented in Figure 1 for each of the 34 experiments. The precision on the outgoing percent at the outlet was evaluated at about 5% (Frey *et al.* 1993).

Numerical modelling of the flow and sediment transport. The seven geometric and hydraulic combinations were simulated numerically using the *interFoam* solver presented previously. The four geometries were meshed using the *snappyHexMesh* tool (OpenFOAM 2016). 'Cut-cell' type meshes with sides of about 7.5 mm and a height of 2.5 mm were chosen (i.e. a y^+ of the order from 1 to 3), leading to a computational domain composed of 500,000 to 600,000 cells according to the geometry. The velocity was imposed on the inlet face of the structure to reproduce the discharges injected experimentally. The boundary condition at the outlet and on the upper part of the computational domain was an atmospheric pressure. The turbulence model k-ω SST was used with standard wall laws (Versteeg & Malalasekera 2007; OpenFOAM 2016). The convergence of the calculation was checked on the basis of stability with time of the mass balance at the outlet and the field of velocities in the different longitudinal and transversal planes.

The particle tracking model presented above was applied to the seven geometric and hydraulic combinations. For each sand sample, a Rosin–Rammler distribution was interpolated to reproduce the experimental grain size distribution. After having verified that this number was sufficient to obtain statistically representative results, 10,000 particles with a density of 2,650 kg/m^3 were injected into the hydraulic flow. In order to reproduce the injection method used experimentally by Frey *et al.* (1993), the injection surface was defined by a disc 8 mm in diameter placed immediately upstream of the break of slope. The centre of the disc was centred in relation to the side walls and located 10 mm from the bottom of the supply channel. The forces taken into account to calculate the trajectories of the particles were drag force and apparent weight. The turbulent nature of the flow was modelled using the stochastic dispersion model presented previously. A *rebound* condition was used for the inlet and the side walls. An *escape* condition (OpenFOAM 2016) was applied to the outlet and to the atmosphere. Regarding the bottom of the structure, using the *stick* condition was, *a priori*, sufficient since, on the one hand, the sediment depositions observed experimentally were not localised in certain zones of the bottom (Frey *et al.* 1993), and on the other hand, the authors showed that by covering the bottom of the settling basin with particles and by progressively bringing the discharge to its nominal value, the particles did not return to suspended state (no particle collected at the outlet of the structure). The new particle/wall interaction conditions (BSS and BTKE) were, however, used to determine whether one of them permitted obtaining more consistent results than with the *stick* condition or, failing that, verifying that they provided similar results. The boundary conditions used were therefore: *stick*, 'Brownlie BSS', 'Van Rijn BTKE', 'extended Van Rijn BTKE' and a BTKE condition with a fixed coefficient ξ. For the latter condition, the values $\xi = 1$ (Yan *et al.* 2014) and $\xi = 5$ (Bagnold criterion) were studied.

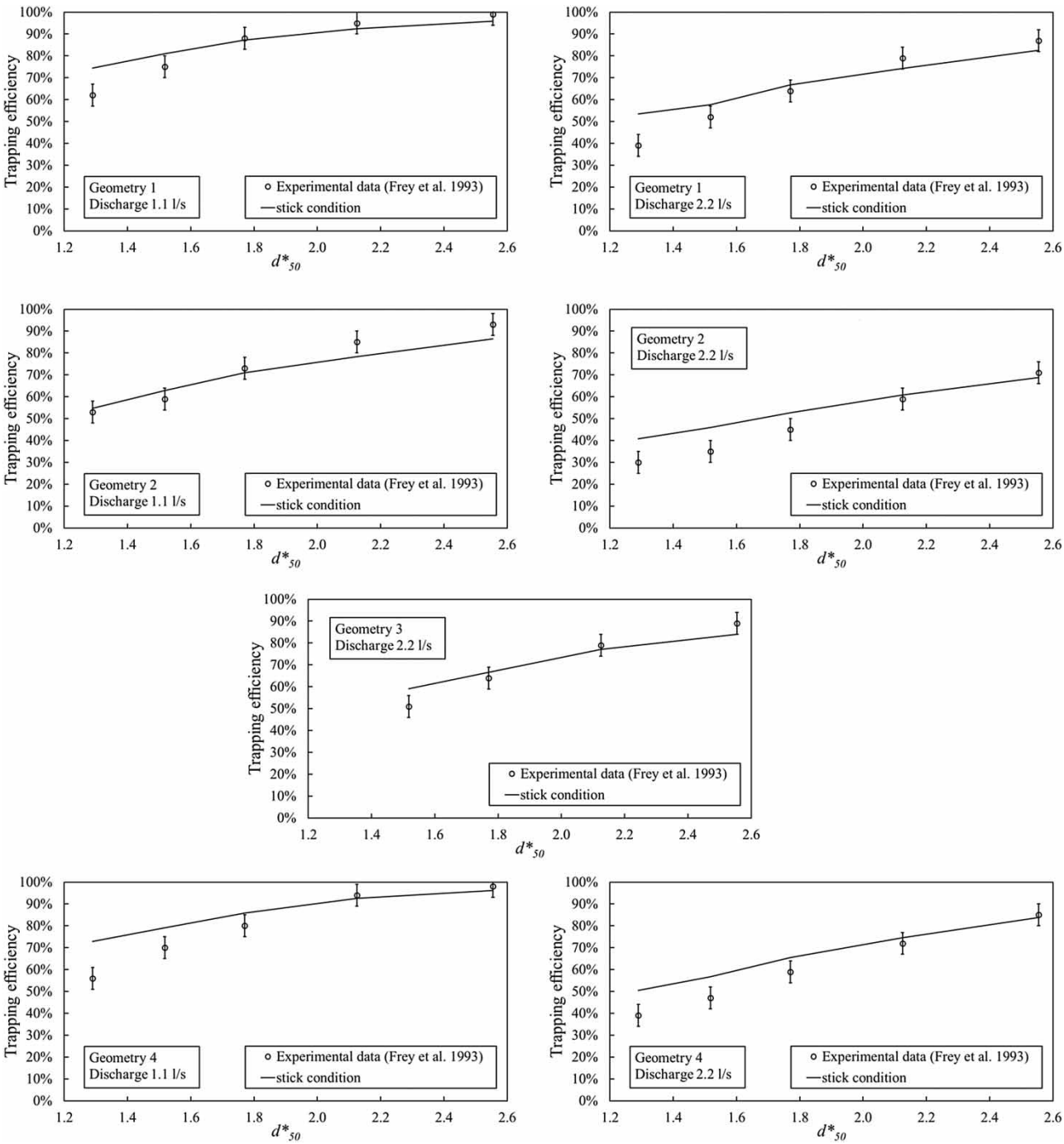

Figure 1 | Comparison of numerical results with the experimental data of Frey *et al.* (1993).

The experiments of Stovin & Saul (1994)

Experimental protocol and results. The experiments conducted by Stovin & Saul (1994) were performed on a scale model of a rectangular basin with Froude similarity (scale 1/15) with a storage basin typically found on combined sewer systems. The shape and dimensions of the structure are described in Stovin & Saul (1994). A range of discharges between 4 and 16 l/s was investigated for two fixed water depths in the basin (0.2 and 0.3 m). The particles injected were crushed olive stones with a density of 1,453 kg/m^3. The grain size distribution ranged from 5 to 150 μm, with

a median diameter of 47 μm. The efficiency of the structure regarding particle trapping efficiency was determined on the basis of the concentration at the outlet and that at the inlet, with these two values being estimated using turbidity measurements. The uncertainty of this method is difficult to quantify, but is probably far greater than that of sieving, in particular due to the turbidity-concentration relation. Three tests were performed for each hydraulic configuration. The experimental results therefore present three efficiency values for a given discharge. The experimental measurements are summarised in Figure 2. Furthermore, the sediment depositions on the bottom of the basin were localised by observations with the naked eye and photographs, then transposed on a sketch for three experiments (Figure 3).

Numeric modelling of the flow and sediment transport. The methodology followed to model the flow and sediment transport is analogous to that presented for modelling the experiments of Frey *et al.* (1993). All the details can be found in Isenmann (2016). For the bottom of the structure, the particle/wall interaction conditions investigated are: *stick*, 'Brownlie BSS', 'Van Rijn BTKE', and 'extended Van Rijn BTKE'. The BTKE conditions with a fixed value of ξ were not used, since a preliminary study of the distribution of the turbulent kinetic energy on the bottom showed that no particle could be deposited given the threshold calculated (Isenmann 2016).

The experiments of Dufresne *et al.* (2009)

Experimental protocol and experimental results. The experiments conducted by Dufresne *et al.* (2009) were performed on a scale model of a rectangular basin. Two configurations were studied: an outlet by a culvert in the lower part of the basin and an outlet by an overflow. The shape and dimensions of the structure are described in Dufresne *et al.* (2009). A range of discharges between 1 and 5 l/s was investigated for different water depths between 8 and 40 cm. The particles injected were white polystyrene beads with a grain size ranging from 350 to 1,400 μm with a median diameter of 738 μm (d^* between 2.5 and 10). The density was evaluated at 1,034 kg/m^3 ($\pm$19 kg/m^3) by pycnometry. At the end of the experiment, the particles settled and recovered at the outlet were reintroduced in a measurement column to evaluate the structure's efficiency. Furthermore, photographs and films of the bottom of the basin were taken for each experiment to track the evolution of the sediment depositions.

Numeric modelling of the flow and sediment transport. The methodology followed to model the flow and sediment transport was analogous with that presented for modelling the experiments of Frey *et al.* (1993) and Stovin & Saul (1994). All the details can be found in Isenmann (2016). The particle/wall interaction conditions studied were: *stick*, 'Brownlie BSS', 'Van Rijn BTKE' and BTKE with a fixed value of ξ (equal to 1 and 5). It should be noted that the 'extended Van Rijn BTKE' condition was equivalent to the 'Van Rijn BTKE' condition for the range of d^* associated with these experiments ($d^*_{min} > 2$). Due to the large standard deviation on the value of the density of the particles in relation to the density of the water (1,034 $\pm$ 19 kg/m^3), two other values were also investigated: 1,015 kg/m^3 (corresponding to the low value of the range) and 1,025 kg/m^3 (corresponding to the intermediate value between the average value and the low value).

RESULTS AND DISCUSSION

Comparison of numerical and experimental results

The experiments of Frey *et al.* (1993)

When all the particles had been deposited or had left the structure via the outlet, the mass percent at the outlet could

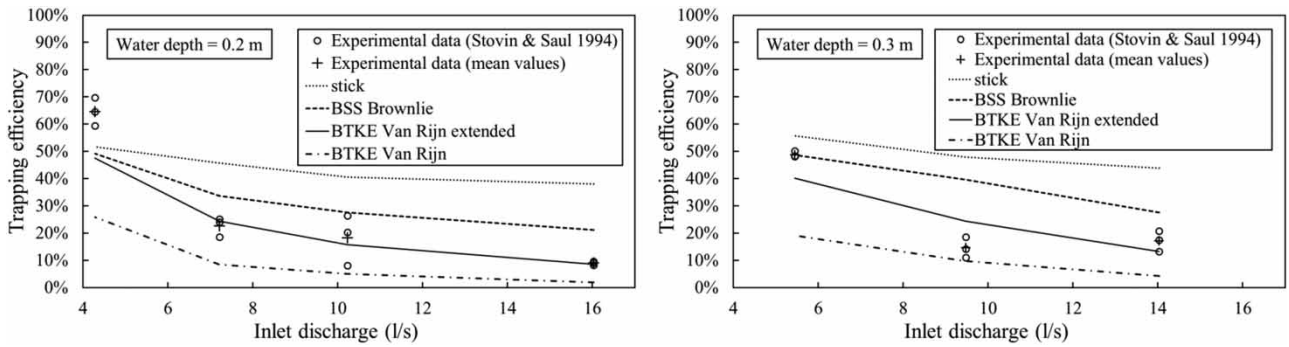

Figure 2 | Comparison of the numerical trapping efficiencies with the experimental data of Stovin & Saul (1994).

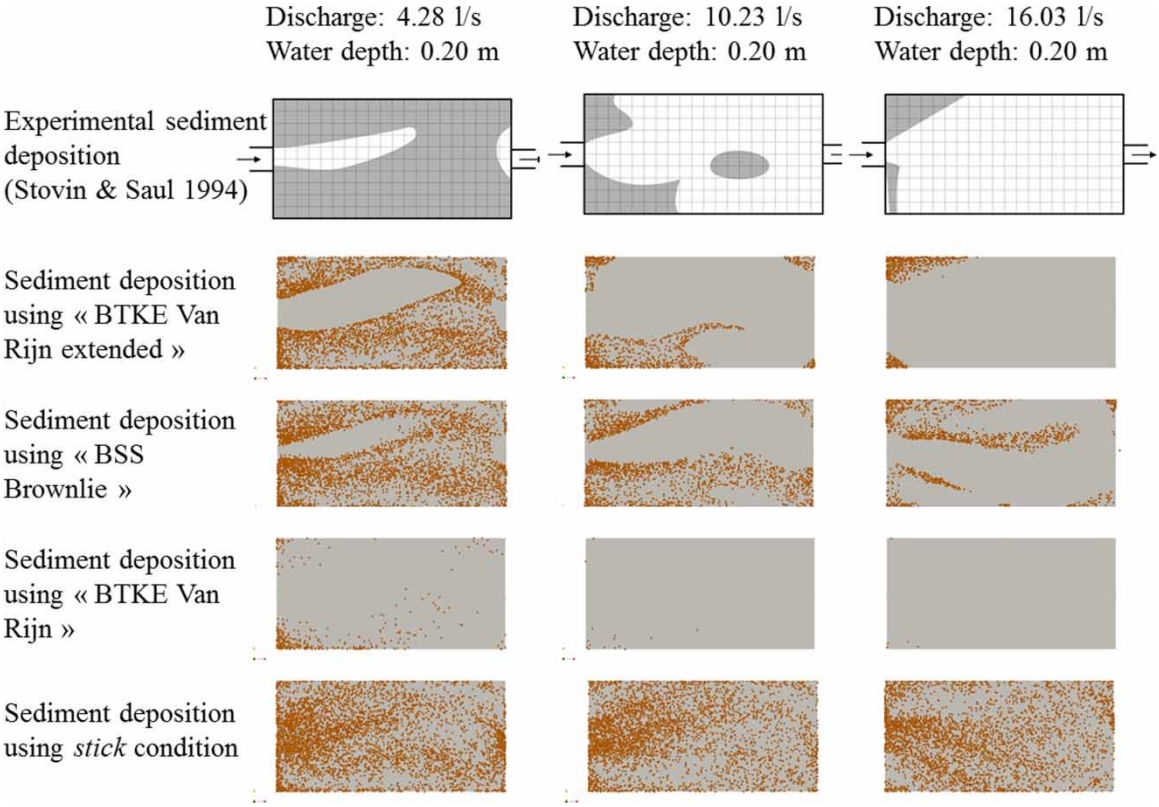

Figure 3 | Comparison of numerical sediment depositions with the experimental data of Stovin & Saul (1994).

be calculated. Figure 1 shows the comparison between the numerical and experimental results for the 34 simulations performed under the *stick* condition. Each graph corresponds to a geometrical and hydraulic configuration for the different sand samples studied. The samples are represented by their median dimensionless diameter d^*_{50}. The absolute variance between the calculated value and that measured experimentally is on average ±6% of the efficiency. The variance is larger for low values of d^*, with a maximum of 17%. Generally, the numerical model faithfully reproduces particle trapping efficiency in the structure, as most of the values were within the experimental error bars. The numerical results obtained for the other particle/wall interaction conditions are not described here, but are available in Isenmann (2016). Nonetheless, it should be emphasised that the 'Brownlie BSS', 'Van Rijn BTKE' and 'extended Van Rijn BTKE' conditions provide similar results to the *stick* condition and are thus well adapted for this case where the sediment deposits cover the whole of the bottom. However, the BTKE conditions using a fixed value of ξ (equal to 1 or 5) appear to be too restrictive regarding the sediment deposition (presence of zones free of sediment) and thus lead to underestimated trapping efficiencies most of the time.

The experiments of Stovin & Saul (1994)

At the end of the simulation, the basin's trapping efficiency was calculated for each of the boundary conditions investigated for the bottom of the structure. Figure 2 shows the comparison of the numerical and experimental efficiencies as a function of the supply discharge for water depths of 0.20 m and 0.30 m. Since the experimental measurements could present a wide range of efficiencies for the same discharge (for example, between 8% and 27% at 11.5 l/s for a water depth of 0.20 m in Figure 2), the variances were calculated in relation to the mean value of the three experimental measurements (represented by a cross in Figure 2).

The results for the trapping efficiency show high sensitivity to the interaction condition used. The *stick* condition leads to an overestimation of efficiency in the region of 20–35% in most cases, except for low discharges. Trapping efficiency was also overestimated with the 'Brownlie BSS' condition, with however a smaller variance with the experimental measurements (about 10–20%). On the contrary, the 'Van Rijn BTKE' condition led to an underestimation of trapping efficiency for all the experiments. The differences with the measurements could reach 30% (low

discharge and water depth of 0.30 m). Lastly, the 'extended Van Rijn BTKE' condition supplied trapping efficiencies that were sometimes higher and sometimes lower than the experimental measurements, with the variance always lower than 10%, except for the lowest discharge (15%).

The other essential point for determining the most efficient interaction condition concerns the location of the sediment deposits at the bottom of the structure. The sediment depositions at the end of the simulation are presented in Figure 3 for each interaction condition, and are compared with the sediment depositions observed by Stovin & Saul (1994). The comparisons are made for the three experiments for which the sediment depositions observed experimentally are available, that is to say, those observed for a water depth of 0.20 m and discharges of 4.28, 10.23 and 16.03 l/s.

The sediment depositions obtained with the *stick* and 'Van Rijn BTKE' conditions confirm the weakness of these conditions, already highlighted when comparing the trapping efficiencies. Indeed, the *stick* condition leads to sediment depositions over the entire bottom and thus does not reproduce the zones of sediment deposition observed experimentally. The 'Van Rijn BTKE' condition strongly underestimates the sediment deposition, or limits it to only a few particles for high discharges. The sediment deposits obtained with the 'Brownlie BSS' condition reproduce the zones of sediment deposition observed for the lowest discharge particularly well. On the other hand, for the other two discharges, a large number of particles were deposited in zones that should be free of any sediment. Lastly, the sediment deposits obtained with the 'extended Van Rijn BTKE' condition are in good agreement with the observations of Stovin & Saul (1994). The zones free of sediment for the low discharge are fairly well reproduced, despite a slight overestimation of the size of the longitudinal strip free of sediment along the main jet. For the intermediate discharge, the sediment deposits in the upstream left and right corners are clearly shown. The isolated deposit in the centre of the basin is, however, averagely reproduced. For the highest discharge, the model reproduces the sediment depositions in the upstream left and right corners, with the rest of the structure remaining free of sediment.

The experiments of Dufresne *et al.* (2009)

The comparison of the numerical and experimental results can be found in Isenmann (2016), only conclusions are presented here.

Whatever the condition of interaction between the particles and the walls, the trapping efficiencies calculated by the model are overestimated in comparison with the experimental measurements. It should be noted however that the relatively high uncertainty on the density of the particles in comparison to that of water ($1{,}034 \pm 19$ kg/m^3) makes the trapping efficiencies calculated very sensitive. In view of this observation, it seems more advisable to use the sediment deposits in the structure as the basis for evaluating the pertinence of the conditions of interaction at the wall. Although the BTKE condition using a fixed value of ξ equal to 1 appears the most pertinent regarding the trapping efficiencies calculated, it nonetheless leads to a poor representation of sediment deposits for most of the experiments (considerable underestimation of the zones of sediment deposition). This condition is therefore unsatisfactory, as it permits reproducing trapping efficiency at the expense of reproducing sediment deposition well. Finally, in spite of the trapping efficiencies calculated that are globally higher than the experimental measurements, the 'Van Rijn BTKE' condition (in this case equivalent to the 'extended Van Rijn BTKE' condition) appears the most pertinent. The preferential zones of sediment deposition are well-reproduced for all the experiments and the trapping efficiencies calculated with densities of 1,015 kg/m^3 and 1,025 kg/m^3 are fairly consistent with the experimental trapping efficiencies, though without considerably degrading the representation of the zones of sediment deposition.

Discussion of trapping efficiency and zones of sediment deposition

The model developed was applied to three series of experiments performed on scale models of basins with a view to verifying the model's capacity to reproduce the phenomena involved in sediment transport in a settling basin. The two essential data for validating the model were the particle trapping efficiency of the structure and the preferential zones of sediment deposition on the bottom.

The model's capacity to reproduce the efficiency of a structure was first verified by comparison with the experimental data of Frey *et al.* (1993). For the 34 experiments covering dimensionless diameters d^* between 0.5 and 5, the mean variance between the trapping efficiencies calculated and measured was about 6%, as most of the values were inside the experimental error bars. Given the hydrodynamic conditions and the properties of the particles, the sediment depositions could occur over the whole bottom of the basin. Therefore the impact of the new interaction conditions regarding the preferential zones of sediment deposition was not studied for these experiments, since

most of them provided the same results as those obtained with the *stick* condition (the two BTKE conditions using a fixed value ξ led to results inconsistent with the experimental observations, thereby demonstrating their limits).

On the contrary, the *stick* condition was poorly adapted in the case where zones free of sediment occurred on the bottom of the structure, such as in the experiments of Stovin & Saul (1994) and Dufresne *et al.* (2009). The new interaction conditions implemented were therefore studied using these two sets of experimental data. Initially, the range of d^* between 0.1 and 2.5 ($d^*_{50} = 0.77$) was investigated on the basis of the experiments of Stovin & Saul (1994). The 'extended Van Rijn BTKE' condition provided satisfactory results, both for the trapping efficiencies and for the preferential zones of sediment deposition on the bottom. The other BTKE conditions, i.e. the 'Van Rijn BTKE' condition and the two BTKE conditions using a fixed value ξ (1 or 5), demonstrated their inability to reproduce the measurements and experimental observations for the range of d^* investigated. The condition based on thresholding the shear stress (Brownlie BSS) permitted the acquisition of acceptable trapping efficiencies although it proved limited for reproducing zones of sediment deposition for strong discharges. Secondly, the range of d^* between 2.5 and 10 ($d^*_{50} \approx 5$) was studied using the experimental data of Dufresne *et al.* (2009). Once again, the 'extended Van Rijn BTKE' condition (equivalent to 'Van Rijn BTKE' for this range of d^*) gave the most satisfactory results. The two BTKE conditions using a fixed value ξ (1 or 5) proved to be incapable of faithfully reproducing the zones of sediment deposition on the bottom, which were either underestimated ($\xi = 1$) or overestimated ($\xi = 5$). The zones of sediment deposition obtained with the 'Brownlie BSS' condition were poorly reproduced, especially for deep water depths in the basin.

Finally, the 'extended Van Rijn BTKE' interaction condition proved to be the most pertinent for d^* between 0.1 and 10. Generally, it permitted the satisfactory reproduction of the particle trapping efficiencies and zones of sediment deposition for the three series of experiments on the scale models of basins.

CONCLUSIONS AND OUTLOOK

The objective of this study was to develop a tool for evaluating the performance of a settling basin in terms of trapping SM (efficiency of the structure). A numerical method using the Euler-Lagrange method was chosen to model flow and sediment transport. A solver for Lagrangian modelling was formulated using the library OpenFOAM®. It was developed for free surface flows, since it utilises the hydrodynamic results of a multiphase solver using a *Volume of Fluid* method.

New conditions of interaction between particles and walls, of BSS and BTKE type, were proposed to determine the threshold values at the scale of the particle. In particular, a new relation was presented to calculate the turbulent kinetic energy threshold as a function of the properties of the particle (diameter and density). This relation was based on the evaluation of $k_c = \xi \cdot w_s^2$ with ξ calculated on the basis of (extended) Van Rijn criteria (1984b) as a function of d^*; and w_s calculated by a balance of forces acting on the particle.

The numerical model was applied to three series of experiments performed on scale models of basins (Frey *et al.* 1993; Stovin & Saul 1994; Dufresne *et al.* 2009) to verify the capacity of the model to reproduce the phenomena involved in sediment transport in a settling basin. The results obtained with the new 'extended Van Rijn BTKE condition' proved satisfactory for the particle trapping efficiency and for the preferential zones of sediment deposition. Indeed, the model reproduced efficiency with an absolute error in the region of 5% in the case of sediment deposits on the whole bottom. In the case of localised sediment deposits, preferential zones were faithfully reproduced and the efficiency was evaluated with an absolute error in the region of 10% (except for particles of very low density).

Finally, a numerical tool is available and validated to evaluate the performances of a settling basin regarding its efficiency for trapping SM. This tool is currently applied in the framework of the SIMPLUV project, one of whose objectives is to develop a prefabricated settling structure. The tool is used to test different shapes and configurations of structure with a view to maximising the amount of material deposited. An experimental phase on a physical model of the settling basin at real scale will reinforce the developments carried out by the numerical tool and lead to validating the model on a real structure (without similitude). The scope of application of the tool is intended to be wider than in the SIMPLUV project. For example, it could be used in the design phase or for the renovation of a larger basin (in the region of several thousand cubic metres) to propose shapes and configurations designed to maximise the trapping of SM or reduce its volume for a given level of performance.

More generally, the scientific outlook for this work is the following. From the numerical standpoint, it will be interesting to proceed with a more in-depth study of the spatial distribution of the sediment deposits. The qualitative comparison (visual) could be completed by a quantitative analysis via, for example, the surface density or another

parameter representative of the thickness of the sediment deposit. From the experimental standpoint, this will require performing measurements that will permit building a database of experimental data on the heights of sediments on the bottoms of basins. Work using this type of measurement, based on an ultrasonic method, started during the experimental campaign of the SIMPLUV project (Isenmann 2016).

REFERENCES

Adamsson, Å., Stovin, V. & Bergdahl, L. 2003 Bed shear stress boundary condition for storage tank sedimentation. *Journal of Environmental Engineering* **129** (7), 651–658.

Adamsson, Å., Bergdahl, L. & Lyngfelt, S. 2005 Measurement and three-dimensional simulation of flow in a rectangular detention tank. *Urban Water Journal* **2** (4), 277–287.

Amsden, A., O'Rourke, P. & Butler, T. 1989 *KIVA-II: A Computer Program for Chemically Reactive Flows with Sprays*. Los Alamos National Laboratory, LA-AA560-MS.

Ashley, R. M., Bertrand-Krajewski, J. L., Hvitved-Jacobsen, T. & Verbanck, M. 2004 *Solids in Sewers: Characteristics, Effects and Control of Sewer Solids and Associated Pollutants*. IWA Publishing, London, UK.

Brownlie, W. R. 1981 *Prediction of Flow Depth and Sediment Discharge in Open Channels, Report No. KH-R-43A*, W. M. Keck Laboratory of Hydraulics and Water Resources, California Institute of Technology, Pasadena, CA, USA.

Buffington, J. 1999 The legend of A. F. shields. *Journal of Hydraulic Engineering* **125** (4), 376–387.

Deshpande, S. S., Anumolu, L. & Trujillo, M. F. 2012 Evaluating the performance of the two-phase flow solver interFoam. *Computational Science & Discovery* **5**, 014016.

Dewals, B., Kantoush, S., Erpicum, S., Pirotton, M. & Schleiss, A. 2008 Experimental and numerical analysis of flow instabilities in rectangular shallow basins. *Environ. Fluid Mech.* **8** (1), 31–54.

Dufresne, M., Vazquez, J., Terfous, A., Ghenaim, A. & Poulet, J. 2009 Experimental investigation and CFD modelling of flow, sedimentation, and solids separation in a combined sewer detention tank. *Computers & Fluids* **38** (5), 1042–1049.

Dufresne, M., Dewals, B., Erpicum, S., Archambeau, P. & Pirotton, M. 2010 Classification of flow patterns in rectangular shallow reservoirs. *Journal of Hydraulic Research* **48** (2), 197–204.

Frey, P., Champagne, J. Y., Morel, R. & Gay, B. 1993 Hydrodynamics fields and solid particles transport in a settling tank. *Journal of Hydraulic Research* **31** (6), 736–776.

Graf, W. H. & Altinakar, M. S. 2000 *Hydraulique Fluviale (Fluvial Hydraulics)*. Presses Polytechniques et Universitaires Romandes, Lausanne, Switzerland.

Hirt, C. W. & Nichols, B. D. 1981 Volume of fluid (VOF) method for the dynamics of free boundaries. *Journal of Computational Physics* **39**, 201–225.

Isenmann, G. 2016 Approche Euler-Lagrange pour la modélisation du transport solide dans les ouvrages de décantation (Euler-Lagrange Approach to Model Sediment Transport in Settling Basin). PhD Thesis, University of Strasbourg, France.

Jarrell-Smith, S. & Friedrich, C. T. 2011 Size and settling velocities of cohesive flocs and suspended sediments aggregates in a trailing suction hopper dredge plume. *Continental Shelf Research* **31**, 550–563.

Maxey, M. R. & Riley, J. J. 1983 Equation of motion for a small rigid sphere in a nonuniform flow. *Physics of Fluids* **26** (4), 883–889.

Morsi, S. A. & Alexander, A. J. 1972 An investigation of particle trajectories in two-phase flow systems. *Journal of Fluid Mechanics* **55**, 196–208.

OpenFOAM 2016 Official OpenFOAM Repository – GitHub. https://github.com/OpenFOAM (accessed 13 January 2017).

Pope, N. D., Widdows, J. & Brinsley, M. D. 2006 Estimation of bed shear stress using the turbulent kinetic energy approach – a comparison of annular and field data. *Cont. Shelf Res* **26**, 959–970.

Rusche, H. 2002 Computational Fluid Dynamics of Dispersed Two-Phase Flows at High Phase Fraction. PhD Thesis, Imperial College of Science, Technology and Medicine, London, UK.

Stovin, V. R. & Saul, A. J. 1994 Sedimentation in storage tank structures. *Water Science and Technology* **29** (1-2), 363–372.

Stovin, V. R. & Saul, A. J. 1996 Efficiency prediction for storage chambers using computational fluid dynamics. *Water Science and Technology* **33** (9), 163–170.

Stovin, V. R. & Saul, A. J. 1998 A computational fluid dynamics (CFD) particle tracking approach to efficiency prediction. *Water Science and Technology* **37** (1), 285–293.

Torres,, A. 2008 Décantation des eaux pluviales dans un ouvrage réel de grande taille: éléments de réflexion pour le suivi et la modélisation (Stormwater Settling Process within a Full-Scale Sedimentation System: Elements of Reflection for Monitoring and Modelling). PhD Thesis, INSA de Lyon, France.

Van Rijn, L. 1984a Sediment transport, part I: bed load transport. *Journal of Hydraulic Engineering* **110** (10), 1431–1455.

Van Rijn, L. 1984b Sediment transport, part II: suspended load transport. *Journal of Hydraulic Engineering* **110** (11), 1613–1638.

Versteeg, H. K. & Malalasekera, W. 2007 *An Introduction to Computational Fluid Dynamics*. Prentice Hall, Harlow, England.

Yan, H., Lipeme Kouyi, G., Gonzalez-Merchan, C., Becouze-Lareure, C., Sebastian, C., Barraud, S. & Bertrand-Krajewski, J. L. 2014 Computational fluid dynamics modelling of flow and particulate contaminants sedimentation in an urban stormwater detention and settling basin. *Environmental Science and Pollution Research* **21** (8), 5347–5356.

First received 13 January 2017; accepted in revised form 8 June 2017. Available online 23 June 2017